Characterization of aging behavior of precipitates and dislocations in copper-based alloys

Shigeo Sato,[1,a)] Yohei Takahashi,[2] Kazuaki Wagatsuma,[1] and Shigeru Suzuki[3]
[1]*Institute for Materials Research, Tohoku University, 2-1-1 Katahira, Sendai, Miyagi, Japan*
[2]*Research Department, Nissan ARC, Ltd., 1 Natsushima, Yokosuka, Japan*
[3]*Institute of Multidisciplinary Research for Advanced Materials, Tohoku University, 2-1-Po1 Katahira, Sendai, Miyagi, Japan*

(Received 5 February 2010; accepted 10 February 2010)

The growth of precipitates in a deformed Cu–Ni–Si alloy with an aging treatment and the rearrangement of dislocations were investigated using small-angle X-ray scattering method and XRD line-profile analysis. The small-angle X-ray scattering method was used for characterizing the growth behavior of the precipitates. The results showed that the precipitates grew gradually to a few nanometers in radius when aged under the condition that the alloy exhibited a maximum of the hardness due to precipitation hardening. The growth rate rose from the onset of the overaging, where the hardness started to decrease. The line-profile analysis of copper-based alloy diffraction peaks using modified Williamson–Hall and modified Warren–Averbach procedures yielded a variation in the dislocation densities of the alloy as a function of the aging time. The dislocation density of the alloy before the aging treatment was estimated to be $1.7 \times 10^{15}\ \mathrm{m}^{-2}$ and its high value was held up to the peak-aging time. With the onset of the overaging, however, the dislocation density distinctly decreased by about 1 order of magnitude indicating that a large amount of the dislocations rearranged to release the alloy from the high dislocation-density state. The results suggest that the massive rearrangement of dislocations was accompanied with coarsening of the precipitates. [DOI: 10.1154/1.3416942]

Key words: XRD line-profile analysis, small-angle X-ray scattering, aging treatment, precipitation, dislocation density

I. INTRODUCTION

The copper-based alloy has been extensively used for electronic parts because of their high performance of electrical conductivity and mechanical strength. The highly dispersed nanoscale precipitates, which are formed by an adequate aging treatment, give the alloy a high mechanical performance. On the other hand, the strength is decreased by an overaging treatment where precipitates are coarsened. It has been reported that the peak-aging time, when the maximum strength occurs, is shortened by a cold-rolling treatment prior to the aging treatment (Huang *et al.*, 2003; Markandeya *et al.*, 2005). The cold-rolling treatment is essential to introduce crystal defects as a nucleation site of the precipitates. However, the shortened aging time is not necessarily favorable for obtaining a high electrical property because dissolved elements in the alloy, which generally decrease the electrical conductivity of the alloy, should be precipitated in the copper matrix. Thus, the knowledge on the correlation between the growth behavior of precipitates and crystal defects, in particular, dislocations, in the copper matrix is important.

Small-angle X-ray scattering (SAXS) can be a powerful tool for the quantitative characterization of the growth behavior of the precipitates in the copper-based alloy. Our previous study using the SAXS method suggested that a cold-rolling treatment prior to the aging treatment can stimulate coarsening of the precipitates (Takahashi *et al.*, 2007). This result indicates that a high dislocation density induced by the cold-rolling treatment could have effects on the growth behavior of the precipitates. In order to validate this correlation between the growth behavior of precipitates and the dislocations in the copper matrix, the dislocation density must be estimated quantitatively. Dislocations in a crystal are generally observed using an electron microscope and the characters of dislocations are discussed on the basis of the results. However, it becomes difficult to characterize dislocations under the existence of highly populated precipitates using the direct observation method, which prompts us to apply the X-ray diffraction (XRD) line-profile analysis for characterizing dislocations. The dislocation density can be estimated by a careful analysis of XRD profiles using the modified Williamson–Hall and modified Warren–Averbach methods (Ungar and Borbely, 1996).

In this study, the microstructural evolution of a Cu–Ni–Si alloy with the aging time is investigated using the SAXS method and the XRD line-profile analysis. On the basis of the structural data, the correlation between the growth behavior of the precipitates and changes in the dislocation density are characterized.

II. EXPERIMENTAL

The alloy used in this study was a high-purity Cu–Ni (2.47 wt%)–Si (0.58 wt%). Details of the preparation method of the alloy were reported elsewhere (Suzuki *et al.*, 2006). Briefly, the alloy was prepared from high-purity 6N (99.9999%) copper, 4N nickel, and 6N silicon with a plasma arc melting method. A solution treatment at 1173 K for 10^4 s

[a)]Electronic mail: s.sato@imr.tohoku.ac.jp

 0885-7156/2010/25(2)/104/4/$30.00

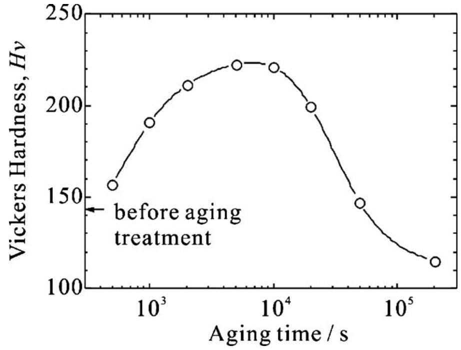

Figure 1. The Vickers hardness of Cu–Ni (2.47 wt%)–Si (0.58 wt%) alloy aged at 720 K as a function of the aging time.

and a subsequent cold rolling by 50% were made, and the alloy was then isothermally aged at 720 K. Figure 1 shows the Vickers hardness of this alloy as a function of the aging time. The hardness rose up to about 5 ks and kept until 10 ks, and then dropped at the aging time of 20 ks. Thus, the peak-age condition of this alloy occurred in the aging times from 5 to 10 ks.

The SAXS measurement was performed using a commercial apparatus (NanoStar, Bruker AXS) equipped with a two-dimensional position sensitive proportional counter. The incident X-ray of Cu $K\alpha$ was monochromated with a cross-coupled Göbel mirror and subsequently collimated by three pinholes. The distance between a sample to the counter was 870 mm to cover the range of the scattering vector q ($q = 4\pi \sin(2\theta/2)/\lambda$) up to 3.0 nm^{-1}, where λ is the X-ray wavelength; 2θ is the scattering angle. Since the background scattering derived from surface imperfections and crystal defects overlaps with the SAXS profile from precipitates, their background contribution was subtracted from the measured scattering profiles using a nonaged sample. The size distribution of precipitates formed in the alloy was obtained from a distance distribution function (DDF), which was calculated from a SAXS profile using the indirect Fourier transform method (Brunner-Popela and Glatter, 1997). A DDF gives a relative number of distances between two points inside a particle as a function of the distance, r.

The XRD measurement was made by a conventional X-ray diffractometer system (X'Pert MPD, PANalytical). Diffraction profiles were measured with a Cu $K\alpha$ radiation in Bragg–Brentano geometry. After eliminating the $K\alpha_2$ component and subtracting the background from the measured profiles, each of the $K\alpha_1$ profiles was fitted to a pseudo-Voigt function. The resulting profile was extracted from this fitted function by the Stokes method (Stokes, 1948) using a diffraction profile of a standard reference material LaB_6 marketed by NIST. The Fourier coefficient was obtained from this estimation.

III. RESULTS AND DISCUSSION

Figure 2 shows SAXS profiles, which were corrected by subtracting the SAXS profile of the nonaged sample, at various aging times. The humps appearing in the SAXS profiles shifted to low-q values with an increase in the aging time suggesting the growth of the precipitates. The calculation fit

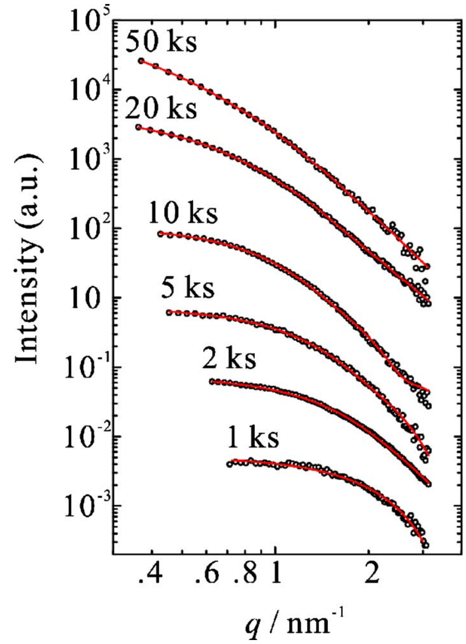

Figure 2. (Color online) Variation in the SAXS profile of the copper alloy aged at 720 K with the aging time. The dots and line denote the experimental and calculated results, respectively.

to the experimental data gave the DDF of the precipitates and the average radius of the precipitates was estimated from the DDF as shown in Figure 3 to represent the average size of the precipitates. The precipitates grew gradually to almost 3 nm in radius at the aging time of 10 ks, which roughly corresponds to the peak-aged condition. Beyond the aging time of 10 ks, the radius of the precipitates increased markedly to about 6 and 9 nm at the aging times of 20 and 50 ks, respectively. This significant coarsening of the precipitates was likely due to the Ostwald ripening (Boistelle and Astier, 1988) inducing the decrease in the number of the precipitates. Therefore, the drop of the Vickers hardness at the aging time of 20 ks can be ascribed to this drastic coarsening of the precipitates.

In order to investigate the effect of the dislocation in the copper matrix on the growth behavior of the precipitates, the diffraction line profiles of the copper matrix were evaluated. Williamson and Hall suggested that the FWHM ($\Delta 2\theta$) of a line profile can be expressed as the sum of the two broadening effects (Williamson and Hall, 1953):

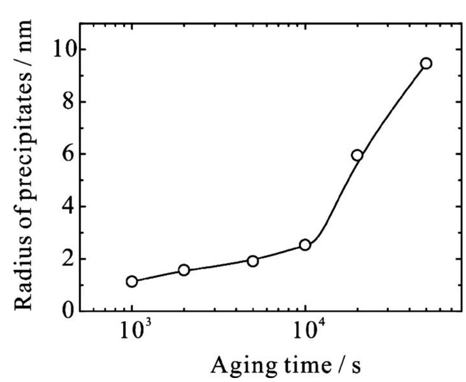

Figure 3. The evolution of the radius of the precipitates with the aging time.

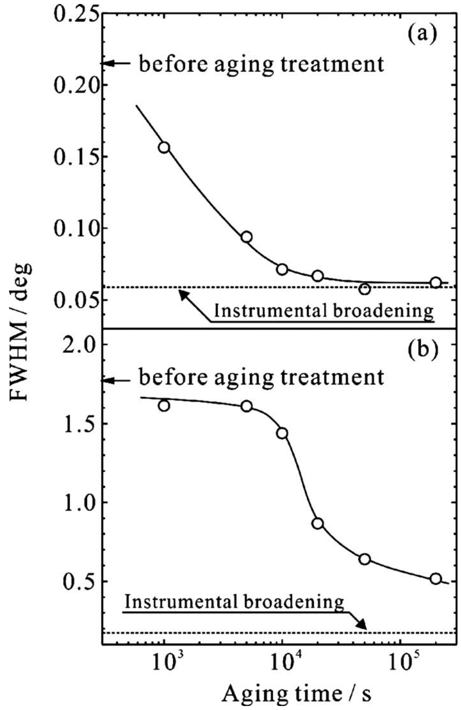

Figure 4. Changes in FWHM of (a) 111 and (b) 420 diffractions of the copper alloy as a function of the aging time.

$$\Delta K = 0.9/D + 2\varepsilon \sin(2\theta/2)/\lambda, \tag{1}$$

where D and ε are an apparent crystallite size and strain, respectively. ΔK is experimentally determined:

$$\Delta K = \Delta 2\theta \cos(2\theta/2)/\lambda. \tag{2}$$

According to Eqs. (1) and (2), the strain contribution becomes larger for the diffraction at higher diffraction angles. Therefore, it is expected that 111 and 420 diffraction lines of the copper-based alloy, observed at about 43.3 and $144.8° 2\theta$, respectively, can be influenced differently by the strain in the copper-based lattice. Figure 4 shows variations in the FWHM of the 111 and 420 diffraction lines as a function of the aging time. The values of the FWHM are estimated from the experimental diffraction peaks, which were corrected by subtracting the $K\alpha_2$ component. The FWHM of the 111 diffraction line, which is less influenced by lattice strain, decreases immediately from the start of the aging treatment, indicating the increase in the crystallite size of the copper crystals. On the other hand, the FWHM of the 420 diffraction line shows only a slight decrease up to an aging time of 10 ks and then decreases rapidly beyond the aging time of 10 ks. These results imply that the strain in the copper crystals was reserved up to the peak-aged condition at 10 ks and relaxed with the progress of the overaging.

The FWHM of a line profile was theoretically evaluated using the modified Williamson–Hall plot:

$$\Delta K = 0.9/D + \sqrt{\pi M^2 b^2/2} \cdot \sqrt{\rho} \cdot (K\langle C\rangle^{1/2}) + O(K\langle C\rangle^{1/2})^2, \tag{3}$$

where $K=2\sin(2\theta/2)/\lambda$; ρ and b are the dislocation density and the Burgers vector, respectively. O is a constant for a higher-order term in $K\langle C\rangle^{1/2}$. $\langle C\rangle$ is a dislocation contrast factor depending on the relative orientations between the Burgers and line vectors of dislocations and the diffraction vector:

$$\langle C\rangle = \langle C_{h00}\rangle(1 - qH^2), \tag{4}$$

where $H^2=(h^2k^2+h^2l^2+k^2l^2)/(h^2+k^2+l^2)^2$ for hkl reflections in cubic crystals; and q is a experimentally obtainable parameter depending on the character of dislocations in the crystals. In estimating $\langle C_{h00}\rangle$, the three elastic constants c_{11}, c_{12}, and c_{44} in the cubic system are required. However, it is not possible to obtain these three elastic constants. On the other hand, it was reported that the value of $\langle C_{h00}\rangle$ is around 0.3 from the theoretical consideration and was 0.304 for pure copper (Ungar *et al.*, 1999). Therefore, the value of $\langle C_{h00}\rangle$ for the present copper-based alloy including minor-alloyed elements can be approximated by the value for pure copper. Figure 5 shows the modified Williamson–Hall plot at several aging times. As expected from Figure 4, the slope of the plot changed little up to the aging time of 10 ks and drastically decreased at the aging time of 20 ks. This suggests that a significant decrease in the dislocation density occurred at the onset of the overaging.

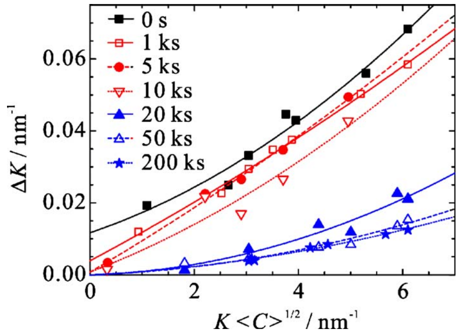

Figure 5. (Color online) The modified Williamson–Hall plots of the copper alloy at various aging times.

In order to estimate the dislocation density in the copper matrix, a further calculation of the line profiles was carried out using the modified Warren–Averbach method:

$$\ln A(L) \cong \ln A^S(L) - (\pi b^2/2) \cdot \rho L^2 \cdot \ln(R_e/L)(K^2\langle C\rangle) + O'(K^2\langle C\rangle)^2, \tag{5}$$

where R_e and L are the effective outer cutoff radius of dis-

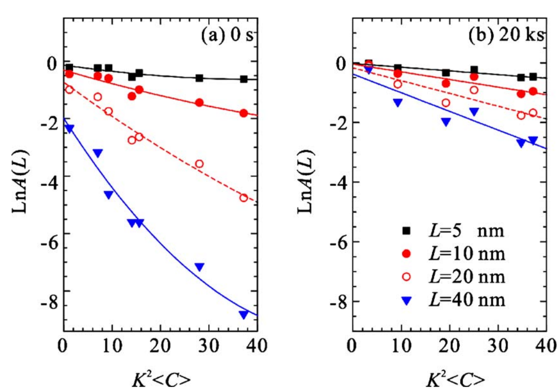

Figure 6. (Color online) The real part of the Fourier coefficients plotted versus $K^2\langle C\rangle$ for different L values according to the modified Warren–Averbach analysis at the aging times of 0 and 20 ks.

https://doi.org/10.1154/1.3416942 Published online by Cambridge University Press

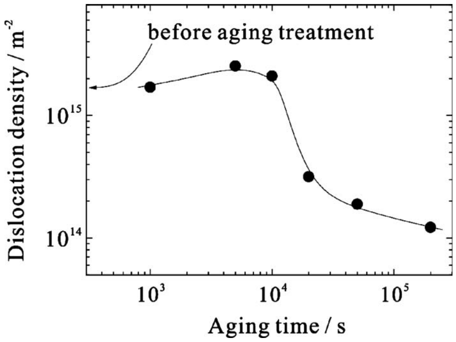

Figure 7. Change in the dislocation density of the copper alloy as a function of the aging time.

locations and the Fourier length, respectively. O' is a constant for a higher-order term of $K^2\langle C\rangle$. Using the dislocation contrast factors led from the modified Williamson–Hall plot, the modified Warren–Averbach plots were obtained as shown in Figure 6. (Only a couple of representative data sets with the aging times of 0 and 20 ks are shown in Figure 6.) The plots for the sample aged for 20 ks (an overaged sample) exhibit much smaller slopes than those of the nonaged sample. This implies that the dislocation density for the overaged sample decreases significantly in comparison to the nonaged sample. The dislocation density as a function of the aging time is shown in Figure 7. Before the aging treatment, the alloy had a high dislocation density of 1.7×10^{15} m^{-2} and the dislocations were introduced by the cold-rolling treatment. As shown in Figure 7, the dislocation density varies with the aging time in accordance with the variation in the growth behavior of precipitates. That is, the dislocation density changes only slightly up to the peak-aging time of 10 ks and then drops by almost 1 order of magnitude at the start of the overaged state of 20 ks. This dependence of the dislocation density on the aging time clearly supports the mechanism, which suggested that the coarsening of precipitates is accompanied with the rearrangement of the dislocation in the copper-based matrix (Takahashi *et al.*, 2007). It should also be noted from Figure 7 that the decrease in the dislocation density becomes relatively smaller at longer aging times beyond 20 ks implying that the dislocations in the copper matrix became relatively more stable by overaging above 20 ks.

IV. CONCLUDING REMARKS

The SAXS analysis showed that the precipitates formed in the Cu–Ni–Si alloy grew gradually to the radius of almost 3 nm by aging at 720 K up to an aging time of 10 ks, where the maximum hardness was obtained. A significant coarsening of the precipitates was caused by aging for more than 20 ks, where the hardness of the alloy started to decrease.

The copper alloy after a solution treatment and a subsequent cold-rolling treatment had a high dislocation density of 1.7×10^{15} m^{-2}. The high dislocation density was maintained up to the peak-aging time of 10 ks. The dislocation density, however, drastically decreased by about 1 order of magnitude at the onset of the overaging (20 ks). It can be concluded that this drastic dislocation rearrangement promoted the coarsening of the precipitates.

Boistelle, R. and Astier, J. P. (**1988**). "Crystallization mechanisms in solution," J. Cryst. Growth **90**, 14–30.

Huang, F., Ma, J., Ning, H., Cao, Y., and Geng, Z. (**2003**). "Precipitation in Cu–Ni–Si–Zn alloy for lead frame," Mater. Lett. **57**, 2135–2139.

Markandeya, R., Nagarjuna, S., and Sarma, D. S. (**2005**). "Effect of prior cold work on age hardening of Cu–4Ti–1Cr alloy," Mater. Sci. Eng., A **404**, 305–313.

Brunner-Popela, J. B. and Glatter, O. (**1997**). "Small-angle scattering of interacting particles. I. Basic principles of a global evaluation technique," J. Appl. Crystallogr. **30**, 431–442.

Stokes, A. R. (**1948**). "A numerical Fourier-analysis method for the correction of widths and shapes of lines on X-ray powder photographs," Proc. Phys. Soc. **61**, 382–391.

Suzuki, S., Shiblitani, N., Mimura, K., Isshiki, M., and Waseda, Y. (**2006**). "Improvement in strength and electrical conductivity of Cu–Ni–Si alloys by aging and cold rolling," J. Alloys Compd. **417**, 116–120.

Takahashi, Y., Sanada, T., Sato, S., Okajima, T., Shinoda, K., and Suzuki, S. (**2007**). "SAXS and XAFS characterization of precipitates in a high-performance Cu–Ni–Si alloy," Mater. Trans. **48**, 101–104.

Ungar, T. and Borbely, A. (**1996**). "The effect of dislocation contrast on x-ray line broadening: A new approach to line profile analysis," Appl. Phys. Lett. **69**, 3173–3175.

Ungar, T., Dragomir, I., Revesz, A., and Borbely, A. (**1999**). "The contrast factors of dislocations in cubic crystals: The dislocation model of strain anisotropy in practice," J. Appl. Crystallogr. **32**, 992–1002.

Williamson, G. K. and Hall, W. H. (**1953**). "X-ray line broadening from filed aluminum and wolfram," Acta Metall. **1**, 22–31.